Inverse Problems for Great Solar Energetic Particle Event: Monitoring by Network Stations and Forecasting

L.I. Dorman [1, 2]

[1] Israel Cosmic Ray and Space Weather Center and Emilio Segre' Observatory, Tel Aviv University, Technion and Israel Space Agency, Israel

[2] Cosmic Ray Department, Pushkov Institute of Terrestrial Magnetism, Ionosphere and Radio Wave Propagation (IZMIRAN), Russian Academy of Sciences, Russia

e-mail: lid@physics.technion.ac.il

Received: 26 November 2008 ; Accepted: 28 December 2008

Abstract. It is well known that energy spectrum of solar energetic particles (SEP), observed by ground-based neutron monitors (NM) and muon telescopes (in the high energy region; the transfer to the space from the ground observations is made by the method of coupling functions) and by detectors on satellites and space-probes (in small energy region), is significantly changed with time (usually from very hard at the beginning of event to very soft at the end of event). The observed spectrum of SEP and its change with time are determined by three main parameters: energy spectrum in source, time of ejection and propagation mode. In the past we considered the first step for forecasting of radiation hazard - the simple isotropic mode of SEP propagation in the interplanetary space. It was shown that on the basis of observational data at several moments of time there could be solved the inverse problem and determined energy spectrum in source, time of ejection and diffusion coefficient in dependence on energy and distance from the Sun. Here we consider the inverse problem for the complicated case, namely, the mode of anisotropic diffusion and kinetic approach. We show that in this case the inverse problem can also be solved, but there is need in neutron monitor data at least from several locations on the Earth. We show that in this case the solution of inverse problem starts to work well sufficiently earlier than solution for isotropic diffusion, but after 20-25 minutes both solutions give about the same results. It is important that obtained results and reality of used model can be controlled by independent data on SEP energy spectrum in other moments of time (is not used at solving of inverse problem). On the basis of obtained results one can estimate the total release energy in the SEP event and radiation environment in the inner heliosphere, the magnetosphere and atmosphere of the Earth during SEP event.

Keywords: solar energetic particles; cosmic rays; neutron monitor; inverse problem; forecasting

1. Introduction

For forecasting of great solar energetic particle (SEP) events we need to solve step by step following problems:

I. On each cosmic ray (CR) stations must work program automatically determining the start of SEP event. This program works many years continuously for neutron monitor (NM) on Mt. Hermon. The description of algorithms and calculations of probability of false and missed alerts on the start of SEP in dependence on amplitude of CR increase are carried out in Sections 2-4.

II. After determining of the start of SEP event, must begin to work program determining the spectrum of SEP out of the Earth's magnetosphere for each moment of time by using method of coupling functions (for algorithms, see: Section 5; method was described in details in Chapter 3 of book [1]).

III. The next step is much more complicated: on the basis of obtained data on SEP energy spectrum in the frame of simple model of isotropic diffusion to determine parameters of propagation, source function and start of acceleration and ejection of solar CR into interplanetary space. This model worked well only after one-two scatterings of SEP in space when the SEP distribution became about isotropic, i.e. after about 15-20 min after ejections of SEP from solar corona. In this case for forecasting of total radiation hazard may be used only one or few NM (see: Sections 6-8).

IV. To extrapolate obtained SEP spectrum from high energies (few GeV on the basis of NM observations) to small energies (hundreds MeV) it is also necessary to use through Internet available one-minute data obtained on-line on satellites (see: Section 9).

V. For earlier warning of radiation hazard from great SEP events it is necessary to use more complicated mode of propagation which describes well the earliest stages of propagation based on kinetic equation and anisotropic diffusion approaches (see: Sections 10-15).

2. The method of automatically search of the start of great SEP event

Let us consider the problem of automatic searching for the start of great SEP event. The determination of increasing flux is made by comparison with intensity averaged from 120 to 61 minutes before the present Z-th one-minute data. For each Z minute data, the program "SEP-Search-1-min" starts, which for both independent channels A and B and for each Z-th minute, determines the values

$$D_{A1Z} = \left[\ln\left(I_{AZ}\right) - \sum_{k=Z-120}^{k=Z-60} \ln\left(I_{Ak}\right) / 60 \right] \Big/ \sigma_1 , \qquad (1)$$

$$D_{B1Z} = \left[\ln\left(I_{BZ}\right) - \sum_{k=Z-120}^{k=Z-60} \ln\left(I_{Bk}\right) / 60 \right] \Big/ \sigma_1 , \qquad (2)$$

where I_{Ak} and I_{Bk} are one-minute total intensities in the sections of neutron super- monitor *A* and *B*.

If simultaneously

$$D_{A1Z} \geq 2.5, \; D_{B1Z} \geq 2.5, \qquad (3)$$

the program "SEP-Search-1-min" repeats the calculation for the next Z+1-th minute and if Eq. 3 is satisfied again, the onset of great SEP is established and the program "SEP-Research/Spectrum" starts. In Fig. 1 shows the picture from our Internet site, upgraded each minute.

3. The probability of false alarms

Because the probability function $\Phi(2.5) = 0.9876$, then the probability of an accidental increase with amplitude more than 2.5σ in one channel will be $(1-\Phi(2.5))/2 = 0.0062 \ \mathrm{min}^{-1}$, that means one in 161.3 min (in one day we expect 8.93 accidental increases in one channel). The probability of accidental increases simultaneously in both channels will be $((1-\Phi(2.5))/2)^2 = 3.845\times10^{-5} \ \mathrm{min}^{-1}$ that means one in 26007 min ≈ 18 days. The probability that the increases of 2.5σ will be accidental in both channels in two successive minutes is equal to $((1-\Phi(2.5))/2)^4 = 1.478\times10^{-9} \ \mathrm{min}^{-1}$ that means one in $6.76\cdot10^8$ min ≈1286 years. If this false alarm (one in about 1300 years) is sent, it is not dangerous, because the first alarm is preliminary and can be cancelled if in the third successive minute there is no increase in both channels bigger than 2.5σ (it is not excluded that in the third minute there will be also an accidental increase, but the probability of this false alarm is negligible: $((1-\Phi(2.5))/2)^6 = 5.685\times10^{-14} \ \mathrm{min}^{-1}$ that means one in 3.34×10^7 years). It should be noted that the false alarm can be sent also in the case of solar neutron event (which really is not dangerous for electronics in spacecrafts or for astronaut's health), but this event usually is very short (only few minutes) and this alarm will be automatically canceled in the successive minute after the end of a solar neutron event.

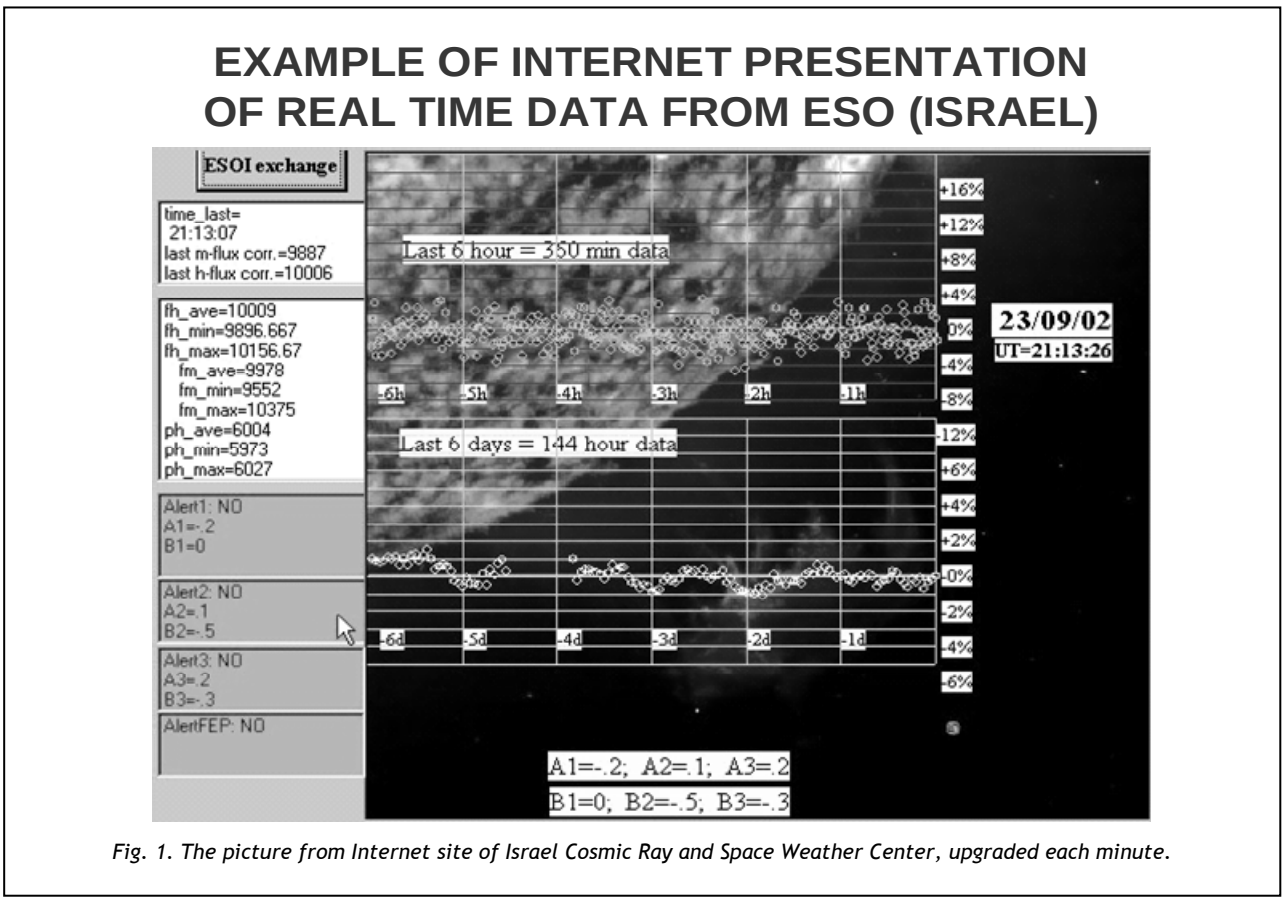

Fig. 1. The picture from Internet site of Israel Cosmic Ray and Space Weather Center, upgraded each minute.

4. The probability of missed triggers

The probability of missed triggers very strongly depends on the amplitude of the increase. Let us suppose that, for example, we have a real increase of 7σ (that for ESO corresponds to an increase of about 9.8 %). The trigger will be missed if in any of both channels and in any of both successive minutes if as a result of statistical fluctuations the increase of intensity is less than 2.5σ. For this, the statistical fluctuation must be negative with amplitude more than 4.5σ. The probability of this negative fluctuation in one channel in one minute is equal to $(1-\Phi(4.5))/2 = 3.39\times10^{-6}\,\mathrm{min}^{-1}$, and the probability of missed trigger for two successive minutes of observation simultaneously in two channels is 4 times larger: 1.36×10^{-5}. It means that missed trigger is expected only one per about 70000 events.

5. On-line determining of the SEP spectrum

The observed CR variation $\delta I_m(R_c,t) \equiv \Delta I_m(R_c,t)/I_{mo}(R_c)$ of some component *m* can be described in the first approximation by function $F_m(R_c,\gamma)$:

$$\delta I_m(R_c,t) = b(t)F_m(R_c,\gamma(t)) \tag{4}$$

where *m* = tot, 1, 2, 3, 4, 5, 6, 7, ≥8 for neutron monitor data (but can denote also the data obtained by muon telescopes at different zenith angles and data from satellites), and

$$F_m(R_c,\gamma) = a_m k_m\left(1-\exp\left(-a_m R_c^{-k_m}\right)\right)^{-1}\int_{R_c}^{\infty} R^{-(k_m+1+\gamma)}\exp\left(-a_m R^{-k_m}\right)dR \tag{5}$$

is the known function. Let us compare data for two components *m* and *n*. According to Eq.(4) we obtain

$$\delta I_m(R_c,t)/\delta I_n(R_c,t) = \Psi_{mn}(R_c,\gamma), \tag{6}$$

where

$$\Psi_{mn}(R_c,\gamma) = F_m(R_c,\gamma)/F_n(R_c,\gamma) \tag{7}$$

are calculated by using Eq.(5). Comparison of experimental results with function $\Psi_{mn}(R_c,\gamma)$ according to Eq.(6) gives the value of $\gamma(t)$, and then from Eq.(4) the value of the parameter $b(t)$.

6. On-line determination simultaneously time of ejection, diffusion coefficient and SEP spectrum in source

We suppose that the time variation of SEP flux and energy spectrum can be described in the first approximation by the solution of isotropic diffusion from the pointing instantaneous source described by function $Q(R,r,t) = N_o(R)\delta(r)\delta(t)$.

In this case the expected SEP rigidity spectrum on the distance *r* from the Sun at the time *t* after ejection will be

$$N(R,r,t) = N_o(R)\times\left[2\pi^{3/2}\left(K(R)t\right)^{3/2}\right]^{-1}\times\exp\left(-\frac{r^2}{4K(R)t}\right) \tag{8}$$

where $N_o(R)$ is the rigidity spectrum of total number of SEP in the source, *t* is the time relative to the time of ejection and $K(R)$ is the diffusion coefficient in the interplanetary space in the period of SEP event. Let us suppose that the time of ejection T_e, diffusion coefficient $K(R)$, and the source spectrum $N_o(R)$ are unknown. In this case for determining on-line simultaneously time of ejection T_e, diffusion coefficient $K(R)$ and SEP spectrum in source $N_o(R)$ we need information on observed SEP spectrum at least in three moments of time T_1, T_2 and T_3 (all times *T* are in UT scale). In this case for times after SEP ejection from the Sun into solar wind we will have:

$$t_1 = T_1 - T_e = x,\; t_2 = T_2 - T_1 + x,\; t_3 = T_3 - T_1 + x \tag{9}$$

where T_2-T_1 and T_3-T_1 are known values and x is unknown value what we need to determine at the first. From three equations of type Eq. (8), but for times t_1, t_2 and t_3 we obtain

$$\frac{T_2-T_1}{x(T_2-T_1+x)} = -\frac{4K(R)}{r_1^2}\times\ln\left\{\frac{b(T_1)}{b(T_2)}\left(x/(T_2-T_1+x)\right)^{3/2}R^{-[\gamma(T_1)-\gamma(T_2)]}\right\} \tag{10}$$

$$\frac{T_3-T_1}{x(T_3-T_1+x)} = -\frac{4K(R)}{r_1^2}\times\ln\left\{\frac{b(T_1)}{b(T_3)}\left(x/(T_3-T_1+x)\right)^{3/2}R^{-[\gamma(T_1)-\gamma(T_3)]}\right\} \tag{11}$$

After dividing Eq. (10) and Eq. (11) we obtain

$$x = \left[(T_2-T_1)\Psi - (T_3-T_1)\right]/(1-\Psi) \tag{12}$$

where

$$\Psi = \frac{T_3-T_1}{T_2-T_1}\times\frac{\ln\left\{\frac{b(T_1)}{b(T_2)}\left(x/(T_2-T_1+x)\right)^{3/2}R^{\gamma(T_2)-\gamma(T_1)}\right\}}{\ln\left\{\frac{b(T_1)}{b(T_3)}\left(x/(T_3-T_1+x)\right)^{3/2}R^{\gamma(T_3)-\gamma(T_1)}\right\}} \tag{13}$$

Eq. (12) can be solved by the iteration method: as the first approximation, we can use $x_1 = T_1 - T_e \approx 500$ sec which is a minimum time of relativistic particles propagation from the Sun to the Earth's orbit. Then by Eq. (13) we determine $\Psi(x_1)$ and by Eq. (12) determine the second approximation x_2, and so on. After solving Eq. (12) and determining the time of ejection, we easily compute diffusion coefficient from Eq. (10) or Eq. (11):

$$-K(R) = \frac{r_1^2(T_2-T_1)/4x(T_2-T_1+x)}{\ln\left\{\frac{b(T_1)}{b(T_2)}\left(x/(T_2-T_1+x)\right)^{3/2}R^{\gamma(T_2)-\gamma(T_1)}\right\}} = \frac{r_1^2(T_3-T_1)/4x(T_3-T_1+x)}{\ln\left\{\frac{b(T_1)}{b(T_3)}\left(x/(T_3-T_1+x)\right)^{3/2}R^{\gamma(T_3)-\gamma(T_1)}\right\}} \tag{14}$$

After determining the time of ejection and diffusion coefficient, it is very easy to determine the SEP spectrum in source:

$$N_o(R)=2\pi^{1/2}b(t_1)R^{-\gamma(t_1)}D_o(R)\times\left(K(R)t_1\right)^{3/2}\exp\left(r_1^2/(4K(R)t_1)\right) \quad (15)$$
$$=2\pi^{1/2}b(t_2)R^{-\gamma(t_2)}D_o(R)\times\left(K(R)t_2\right)^{3/2}\exp\left(r_1^2/(4K(R)t_2)\right)$$
$$=2\pi^{1/2}b(t_3)R^{-\gamma(t_3)}D_o(R)\times\left(K(R)t_3\right)^{3/2}\exp\left(r_1^2/(4K(R)t_3)\right)$$

7. The inverse problem for the case when the diffusion coefficient depends from the distance to the Sun (isotropic diffusion)

Let us suppose that the diffusion coefficient $K(R,r)=K_1(R)\times(r/r_1)^{\beta}$. In this case (see the well-known book of Parker, 1963)

$$n(R,r,t)=\frac{N_o(R)\times r_1^{3\beta/(2-\beta)}(K_1(R)t)^{-3/(2-\beta)}}{(2-\beta)^{(4+\beta)/(2-\beta)}\Gamma(3/(2-\beta))}\times\exp\left(-\frac{r_1^{\beta}r^{2-\beta}}{(2-\beta)^2K_1(R)t}\right) \quad (16)$$

If we know n_1,n_2,n_3 at moments of time t_1,t_2,t_3, the final solutions for β, $K_1(R)$, and $N_o(R)$ will be

$$\beta=2-3\left[(\ln(t_2/t_1))-\frac{t_3(t_2-t_1)}{t_2(t_3-t_1)}\ln(t_3/t_1)\right]\times\left[(\ln(n_1/n_2))-\frac{t_3(t_2-t_1)}{t_2(t_3-t_1)}\ln(n_1/n_3)\right]^{-1}, \quad (17)$$

$$K_1(R)=\frac{r_1^2\left(t_1^{-1}-t_2^{-1}\right)}{3(2-\beta)\ln(t_2/t_1)-(2-\beta)^2\ln(n_1/n_2)}=\frac{r_1^2\left(t_1^{-1}-t_3^{-1}\right)}{3(2-\beta)\ln(t_3/t_1)-(2-\beta)^2\ln(n_1/n_3)} \quad (18)$$

$$N_o(R)=n_1(2-\beta)^{(4+\beta)/(2-\beta)}\Gamma(3/(2-\beta))r_1^{-3\beta/(2-\beta)}(K_1(R)t_k)^{3/(2-\beta)}\times\exp\left(\frac{r_1^2}{(2-\beta)^2K_1(R)t_k}\right) \quad (19)$$

In the last Eq. (19) index k = 1, 2 or 3.

8. SEP forecasting by using only NM data

By using of the SEP event first few minutes of NM data we can determine by Eq. (17)–(19) effective parameters β, $K_1(R)$, and $N_o(R)$, corresponding to the rigidity about 7–10 GV, and then by Eq.(16) we determine the forecasting curve of expected SEP flux behavior for total neutron intensity. We compare this curve with time variation of observed total neutron intensity. Really we use data for more than three moments of time by fitting obtained results in comparison with experimental data to reach the minimal residual (see Fig. 2, which contains 8 panels for time moments t = 110 min up to t = 220 min after 10.00 UT of 29 September, 1989).

From Fig. 2 it can be seen that using only the first few minutes of NM data (t = 110 min) is not enough: the obtained curve forecasts too low intensity. For t = 115 min the forecast shows little bigger intensity, but it also is not enough. Only for t = 120 min (15 minutes after beginning) and later, up to t = 140 min (35 minutes after beginning) we obtain almost stable forecast with good agreement with observed CR intensity (with accuracy of about ± 10 %).

9. Forecasting by using both NM and satellite data

All described above results, based on NM on-line data, reflect the situation in SEP behavior in the high energy (more than few GeV) region. For extrapolation of these results to the low energy interval (dangerous for space-probes and satellites), we use satellite on-line data available through the Internet. The problem is how to extrapolate the SEP energy spectrum from high NM energies to very low energies detected in GOES satellite. The main idea of this extrapolation is as following: the source function, time of ejection and diffusion coefficient in both energy ranges are the same. The source function relative to time and space is δ–function, and relative to energy is power function with an energy-

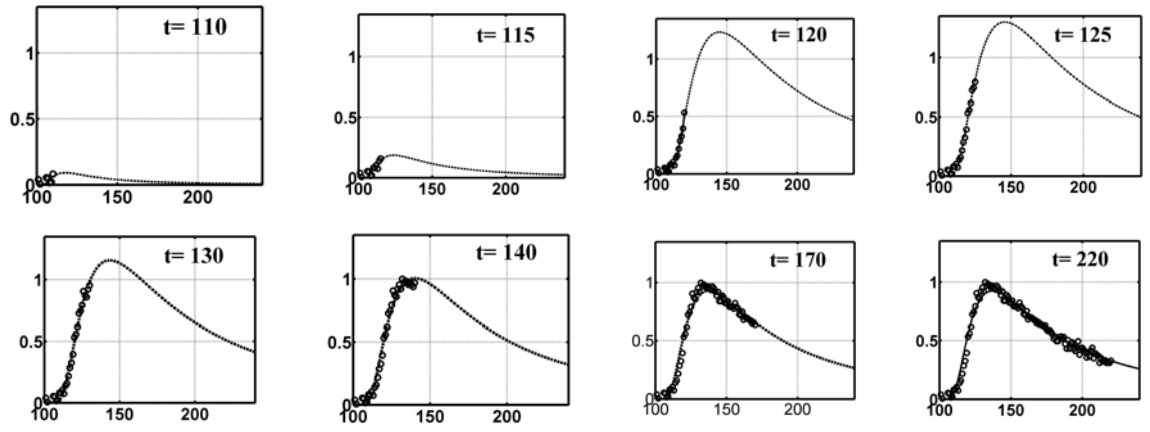

Fig. 2. Calculation on line parameters β, $K_1(R)$, and $N_o(R)$ and forecasting of total neutron intensity (time t is in minutes after 10.00 UT of September 29, 1989; curves – forecasting, circles – observed total neutron intensity).

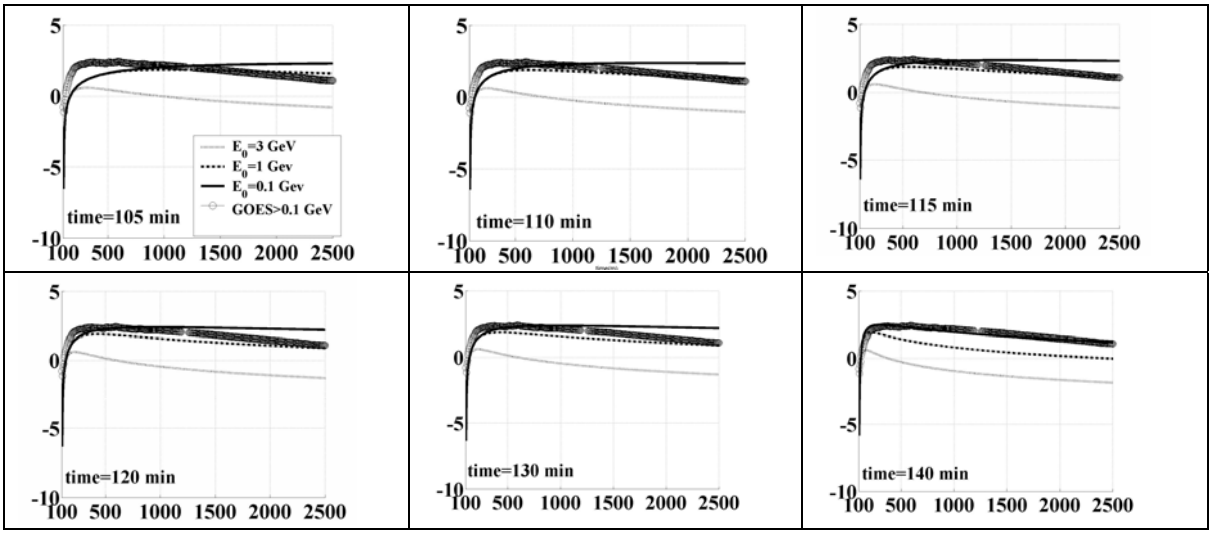

Fig. 3. Predicted SEP integral fluxes for $E_k \geq E_o = 0.1GeV$, $E_k \geq E_o = 1GeV$, $E_k \geq E_o = 3GeV$. *The forecasted integral flux for* $E_k \geq E_o = 0.1GeV$ *we compare with observed fluxes for* $E_k \geq 100MeV$ *on GOES satellite. The ordinate is log₁₀ of SEP integral flux (in cm⁻²sec⁻¹sr⁻¹), and the abscissa is time in minutes from 10.00 UT of September 29, 1989.*

dependent index γ ($\gamma = \gamma_o + \ln(E_k/E_{ko})$ with maximum at $E_{k\max} = E_{ko}\exp(-\gamma_o)$:

$$N_o(R,T) = \delta(T - T_e) \times R^{-(\gamma_o + \ln(E_k/E_{ko}))}. \quad (20)$$

In Fig. 3 there are shown results based on the NM and satellite data of forecasting of expected SEP fluxes also in small energy intervals and comparison with observation satellite data.

From Fig. 3 it can be seen that by using on-line data from ground NM in the high-energy range and from satellites in the low-energy range during the first 30-40 minutes after the start of the SEP event, it is possible to predict the expected SEP integral fluxes for different energies up to a few days ahead.

10. The case of kinetic and anisotropic diffusion approaches: the matter of problem

From consideration of isotropic diffusion in Sections 6-8 we can see that in this case the model starts to work well only after about 15-20 minutes from the real start of event. It means that the used above model of isotropic diffusion cannot adequately describe the solar CR propagation at the beginning of event. To make more exact and earlier forecast it is important to use also data of these beginning minutes. As we mentioned in Abstract, for this we need to use the approach of anisotropic diffusion and kinetic approach. These approaches were considered in details in Chapter 2 of book [2]. Here we will consider principles of solving this very important for practice and very complicated inverse problem on the basis of synchronically working network of neutron monitors with one-minute real data collecting. Our research will be based mainly on theoretical works [3-6].

According to [5], in the theoretical consideration the regular IMF is taken to be homogeneous. Nevertheless, the formation of an initial angle distribution of particles into narrow stream along the regular IMF [7] owed to the magnetic focusing of force-lines near the Sun is included (see: below). Thus, evolution of the particle distribution function $f(y,\tau,\mu)$ follows from the kinetic equation written in the drift approximation, in which the particle scattering on stable magnetic inhomogeneities is supposed to be isotropic [4]:

$$\partial_\tau f + \mu\partial_y f + f - \frac{1}{2}\int_{-1}^{1} f d\mu = \frac{\nu_S}{\nu}\delta(y)\delta(\tau)\varphi(\mu) \quad (21)$$

where *y* and *τ* are the coordinate along regular IMF and the time, respectively (in the dimensionless units $y = z\nu_s/v$, $\tau = \nu_s t$; ν_s is the collision frequency of particles with the magnetic clouds; z is the coordinate along the IMF), $\mu = \cos\theta$, θ is the particle pitch-angle. The right-hand side of Eq. (21) describes an instantaneous injection of CR particles with an initial angular distribution

$$\varphi(\mu) = \frac{a_\mu \Delta_\mu}{2\left(\Delta_\mu^2 + (\mu - \mu_o)^2\right)} \quad (22)$$

where $\mu \in (-1, 1)$. The value of the constant a_μ, which depends on a maximal value direction of μ_o and a width Δ_μ, can be found from the normalization condition, $\int_{-1}^{1}\varphi(\mu)d\mu = 1$, and it is equal to

$$a_\mu = 2\left(\arctan\frac{1-\mu_o}{\Delta_\mu} + \arctan\frac{1+\mu_o}{\Delta_\mu}\right)^{-1} \quad (23)$$

Owing to the focusing effect in the IMF mentioned, μ_o and Δ_μ have values equal to 1 and 0.01, respectively (see numerical estimations by [3]).

11. Pitch-angle response function for neutron monitors

In [5] there is used the pitch-angle response function for neutron monitors $\psi(\lambda)$ which is similar to $\varphi(\mu)$ in which μ has to be replaced by λ (λ is the pitch-angle of an asymptotic NM direction related to the regular IMF direction). The value of λ_o corresponds to the angle of a maximal sensitivity of detector, the parameter Δ_λ characterizes a width of directional diagram of the neutron monitors.

12. Time-finite injection

According to [5], an intensity enhancement of the registered by neutron monitors solar energetic particles arises suddenly at $\tau = y$ for a δ-like particle injection, and a width of the impulse peak connected with arriving of the first particles is very short. Usually one needs to suppose, based on the description of measured temporal profiles of past solar proton events, that the injection of high energy particles into the interplanetary medium has a finite duration, which is caused mainly by the propagation of accelerated particles in the solar corona [7, 8].

The injection of accelerated particles from the source into the IMF during a finite time can be represented by the following time injection function:

$$\chi(\tau) = \nu_o^2 \tau \exp(-\nu_o \tau), \quad (24)$$

where the dimensionless quantity ν_o^{-1} is an unique parameter, which characterizes the mean duration of the injection as well as the instant of maximum at $\tau_m = \nu_o^{-1}$. It was assumed that τ is measured in the dimensionless quantity $\tau = t\nu_s = \nu t/\Lambda$, where Λ is the particle mean path. It is also reasonable to suppose that the duration of the emission by that "particle source" of the lower energy particles is longer, so the quantity ν_o will be dependent on the particle rigidity. Building all these 'weight' functions above into the consideration, a detector will register

$$G(y,\tau) = \int_0^\tau d\xi \int_{-1}^{1} d\mu \chi(\tau-\xi) f(y,\xi,\mu) \psi(\mu). \quad (25)$$

13. Three parts of resulting solution

The solution $G(y,\tau)$, described by Eq. (25), has been obtained in [3] using the method of the direct and inverse Fourier–Laplace transform and it consists of three terms:

$$G(y,\tau) = G_{us}(y,\tau) + G_s^o(y,\tau) + G_s^d(y,\tau). \quad (26)$$

The first component describes a contribution of the unscattered particles which exponentially decreases with time τ:

$$G_{us}(y,\tau) = \frac{\nu_s \nu_o^2 \exp(-\nu_o \tau)}{\nu} \int_0^\tau \frac{d\xi}{\xi} (\tau-\xi) \varphi\left(\frac{y}{\xi}\right) \psi\left(\frac{y}{\xi}\right) \exp(\xi(\nu_o - 1)) \quad (27)$$

A contribution of the scattered particles can be divided into two parts. One is the non-diffusive term $G_s^o(y,\tau)$, also exponentially decreasing with time, and another term, $G_s^d(y,\tau)$, has a leading meaning in the diffusive limit of $\tau >> 1$. Namely, the non-diffusive term is

$$G_s^o(y,\tau) = \frac{\nu_s \nu_o^2 \exp(-\nu_o \tau)}{8\pi\nu} \left\{ \int_0^{y/\tau} d\eta \Psi(y,\tau,\eta)[S(\tau) - S(y)] + \int_{y/\tau}^{1} d\eta \Psi(y,\tau,\eta)[S(y/\eta) - S(y)] \right\} \quad (28)$$

where

$$\Psi(y,\tau,\eta) = \frac{\exp(y\Lambda(\eta)/2)}{\left((\mu_o-\eta)^2 + \Delta_\mu^2\right)\left((\lambda_o-\eta)^2 + \Delta_\lambda^2\right)} \quad (29)$$

$$S(\xi) \equiv S(\xi; y, \tau, \eta) = \frac{\exp(A)}{A^2 + (\pi\eta/2)^2} \times \{(\beta_1 b_1 + \beta_2 b_2)\cos(\pi(y-\xi\eta)) + (\beta_1 b_2 - \beta_2 b_1)\sin(\pi(y-\xi\eta))\}, \quad (30)$$

In Eqs. (29) and (30) the following denominations are used:

$$A = \nu_o - 1 - \eta\Lambda(\eta), \quad \beta_1 = (\tau-\xi)A + \frac{A^2 - (\pi\eta/2)^2}{A^2 + (\pi\eta/2)^2}, \quad \beta_2 = (\tau-\xi)\frac{\pi\eta}{2} + \frac{\pi\eta A}{A^2 + (\pi\eta/2)^2},$$
$$\Lambda(\eta) = \ln(1-\eta) - \ln(1+\eta), \quad b_1 = \pi(\Delta_\mu a_\mu \Pi_\lambda(\eta) + \Delta_\lambda a_\lambda \Pi_\mu(\eta)),$$
$$b_2 = \Pi_\mu(\eta)\Pi_\lambda(\eta) - \pi^2 \Delta_\mu \Delta_\lambda a_\mu a_\lambda, \quad \Pi_\mu(\eta) = 2(\mu_o - \eta) + \Delta_\mu(2\alpha_\mu + a_\mu \Lambda(\eta)),$$
$$\alpha_\mu = \frac{a_\mu}{4}\left[\ln\left(\Delta_\mu^2 + (1+\mu_o^2)^2\right) - \ln\left(\Delta_\mu^2 + (1-\mu_o^2)^2\right)\right]. \quad (31)$$

The last (diffusive non-vanishing) term in Eq.(26) has a sense only for $|y| < \tau$:

$$G_s^d(y,\tau) = \frac{\nu_s \nu_o^2}{4\pi\nu} \int_{-\pi/2}^{\pi/2} \frac{dk}{k^2} \Phi(y,k) \left\{ e^{\tau\kappa} - e^{(y-\tau)\nu_o + y\kappa}[1 + (\tau-y)(\nu_o + \kappa)] \right\} \quad (32)$$

where $\kappa \equiv k\cot k - 1$, and

$$\Phi(y,k) = \frac{(B_\mu B_\lambda - \Gamma_\mu \Gamma_\lambda)\cos(ky) + (B_\mu \Gamma_\lambda + \Gamma_\mu B_\lambda)\sin(ky)}{D_\mu D_\lambda \cos^2 k} \quad (33)$$

$$B_\mu(k) = \Delta_\mu a_\mu (\mu_o^2 + \Delta_\mu^2) k \tan^3 k + (\mu_o^2 - \Delta_\mu^2 + 2\mu\Delta_\mu \alpha_\mu)\tan^2 k - \Delta_\mu a_\mu k \tan k + 1 \quad (34)$$

$$\Gamma_\mu(k)=\left[\left(\mu_o+\Delta_\mu\alpha_\mu\right)\left(\mu_o^2+\Delta_\mu^2\right)\tan^2 k-2\mu_o\Delta_\mu a_\mu k\tan k+\left(\mu_o-\Delta_\mu\alpha_\mu\right)\right]\tan k \quad (35)$$

$$D_\mu(k)=\left[1-\left(\mu_o^2+\Delta_\mu^2\right)\tan^2 k\right]^2+4\mu_o^2\tan^2 k\cdot \quad (36)$$

The expressions for similar quantities $B_\lambda,\Gamma_\lambda,D_\lambda,\Pi_\lambda,a_\lambda,\alpha_\lambda$ follow from the above described expressions by substituting $\mu\to\lambda,\mu_o\to\lambda_o,\Delta_\mu\to\Delta_\lambda\cdot$ Fedorov et al. [5] note that both terms $G_{us}(y,\tau)$ and $G_s^o(y,\tau)$ vanish in the diffusive limit owed to the remaining factor of $\exp(-\nu_o\tau)$; so only $G_s^d(y,\tau)$ gives the main contribution in this limit.

14. Expected temporal profiles for neutron monitors and comparison with observations

According to [5], the main peculiarity of the solar CR events is connected to some neutron monitors (Hobart – HO, Mt. Wellington – WE, Lomnicky Stit – LS) having the narrow peak of the anisotropic stream of the first fast particles; other neutron monitors (Oulu – OU, Apatity – AP, Thule – TH, Durham – DU, Mt. Washington – WA) show a diffusive tail with a wide maximum at a later time, or, show both – the first narrow peak with a second diffusion maximum (South Pole – SP). For example, some selected NM data for the 24 May 1990 are demonstrated in Fig. 4. The time (in min) is measured from the onset of particle injection taken as 20.50 UT of May 24 1990.

Comparison of the NM data with the theoretical prediction based on the kinetic equation solution requires a choice of a "normalizing NM station" and consequent rigidity-dependent re-calculation of input parameters entering into the theoretical profile calculation. The NM station HO was chosen to be that station because it allows to determine the starting parameters at its mean rigidity $\overline{R}$ (HO) = 2.3 GV. This value as well as the others have been calculated by assumption of a particle rigidity spectrum roughly $\propto R^{-5}$ in the initial phase. For other NMs there were taken the following calculated values of the mean rigidity: $\overline{R}_{WE}$ = 2.3 GV, $\overline{R}_{LS}$ = 2.3 GV, $\overline{R}_{OU}$ = 1.0 GV, $\overline{R}_{DU}$ = 2.0 GV, $\overline{R}_{WA}$ = 1.8 GV, and $\overline{R}_{SP}$ = 0.8 GV. The mean rigidity $\overline{R}$ was obtained from trajectory computations for *R* < 10 GV with a step of 0.01 GV by a technique owed to [9]. Each allowed trajectory was assigned by the weight corresponding to the solar proton spectra $\propto R^{-5}$ and the coupling function according to [10, 11]. The geomagnetic field model for trajectory calculations included the IGRF plus the Tsyganenko 89 model [12] for Kp > 5.

The asymptotic directions λ_o for NMs have been obtained by numerical integration of particle motion in the geomagnetic field (by the method described in [9]; see in details in the Chapter 3 of book [13]) for the given epoch at 21:00 hours, and then they were averaged over both the rigidity-dependent response function of NM and the particle rigidity spectrum. For each allowed trajectory the pitch-angle was assigned and the mean value λ_o as well as dispersion Δ_λ were obtained from the histogram of the expected pitch-angle distribution (for the computations there are used vertically incident particles). This simplification is used because:

(a) the contribution to NM count rate is in the geometric approach inversely proportional to cosine of zenith angle,

(b) the main limitation for the trajectory computations is the magnetic field model (Smart et al., 2000),

(c) these computed results [9] can be compared with the vertical cutoff rigidities obtained by other methods [14].

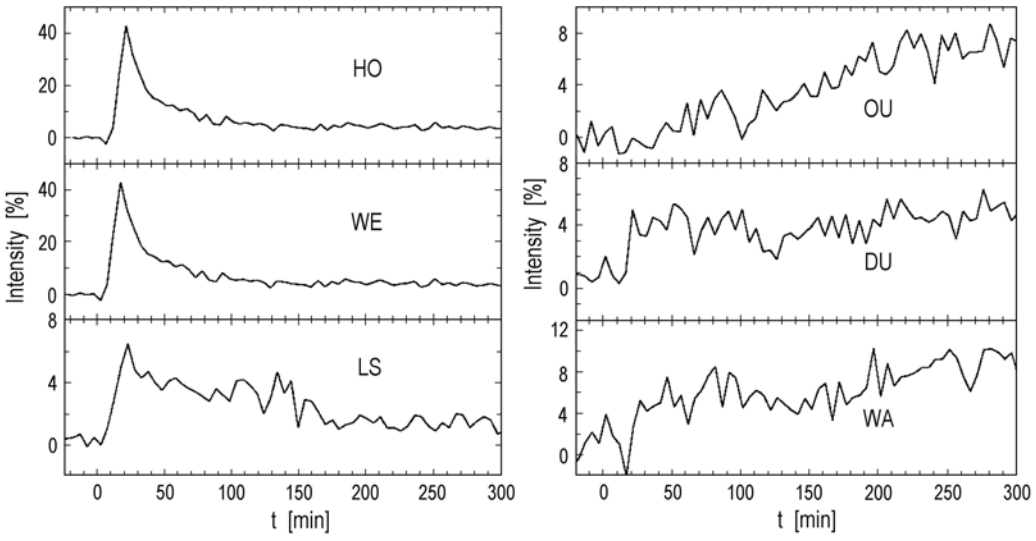

Fig. 4. Two groups of NM records of the event on 24 May 1990. Left - the narrow peak of the anisotropic stream of the first fast particles (HO - Hobart, WE- Mt.Wellington, LS - Lomnicky Stit); right - show a diffusive tail with a wide maximum at a later time (OU - Oulu, DU - Durham, WA- Mt.Washington) [5].

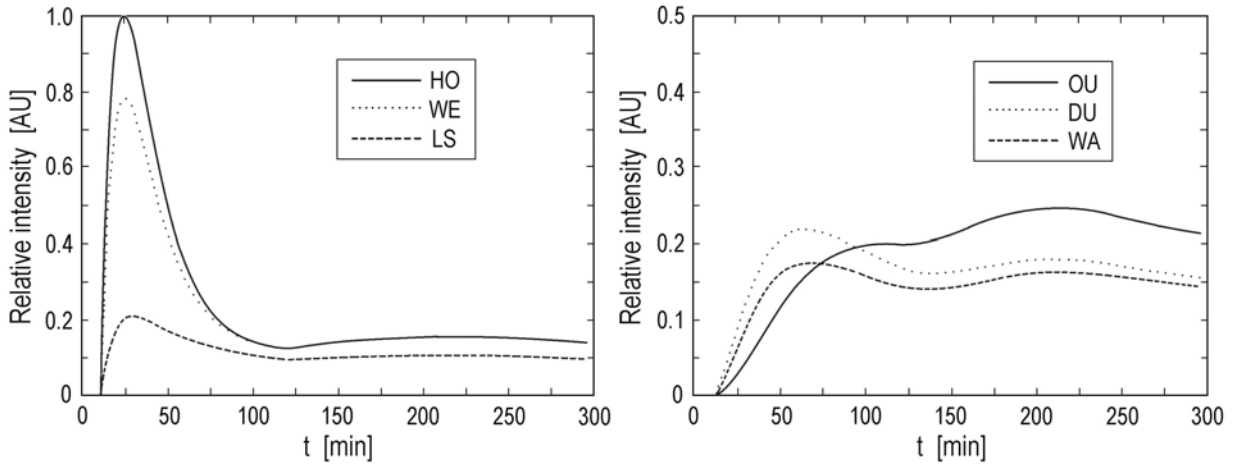

Fig. 5. Theoretical prediction of temporal profiles for the selected NMs using calculated parameters λ_o, $\Delta\lambda$ and mean $\overline{R}$ for each NM. On the ordinate axis there is shown expected intensity relative to HO in maximum [5].

The mean transport path Λ in IMF is supposed to be independent on rigidity for the considered interval of NM sensitivity rigidity. Elementary calculation shows that

$$\nu_o = (10.8/t_m)(\Lambda/z) = 10.8/(yt_m) \quad (37)$$

where z and $y = z/\Lambda$ is the distance of the detector (the Earth) from the source (the Sun) and the dimensionless one, respectively. Therefore the fit of the theoretical curve to experimental data of HO determines $\nu_o = \nu_o(t_m)$ for given y_{HO}. The best fit gives t_m = 12.4 min for y_{HO} = 0.6. Values of ν_o for the other NMs are calculated assuming the rigidity dependence of $t_m \propto \overline{R}^{-\beta}$ using the given value y_{HO}. The spectrum index β characterizes shape of a low energy particle delay in the corona. Fedorov et al. [5] have used the value $\beta = 1$.

For comparison of theoretical dependences with the experimental data the dependence of galactic CR intensity on particle rigidity also has been taken into consideration. Let this dependence be $I_g \propto R^{-\gamma_g}$, where γ_g is galactic CR spectrum index, and the solar CR rigidity dependence at the instant of its injection into IMF is $I_S \propto R^{-\gamma_S}$. All theoretical curves are standardized to a maximum relative to the mean rigidity of HO, i.e., the curve HO has the value 1 in maximum. The multipliers $\left(\overline{R}_{HO}/\overline{R}_i\right)^{\gamma_S-\gamma_g}$ (where *i* = OU, WE, WA, etc.) which take into account the rigidity spectra of galactic CR and SCR, must be used in calculation of the rigidity dependence of the *i* - th NM. The values of the maxima of the theoretical curves of the *i* - th NM are conditioned by the difference of $\Delta\gamma = \gamma_s - \gamma_g$.

The experimental records of temporal profiles can be divided roughly into two groups, one of NMs which in the initial phase (about the first hour after the particle onset) have asymptotic direction near the regular IMF direction (Fig. 4, left panel), and the others whose asymptotic direction differs from it (Fig. 4, right panel). The theoretically predicted temporal profiles for the selected NMs in the model described above are demonstrated in Fig. 5, left and right panels, respectively, using the calculated asymptotic direction for each NM station. This calculation shows that HO and WE have very similar characteristics, λ_o is 0.9 and 0.86, respectively, with $\Delta\lambda$ = −0.26. Station LS has λ_o = 0.34, $\Delta\lambda$ = 0.4. In the second group of NM's, OU, DU, and WA have λ_o = −0.94, −0.9, −0.85 and $\Delta\lambda$ = 0.06, 0.1, 0.3, respectively. Note that Oulu and Apatity give absolutely the same theoretical curves resulting from their similar characteristics and very similar temporal profiles of the event. The last two NMs (DU and WA) experienced small increases at 1–2 hours after onset, as the theory predicts (see Fig. 4 (right panel)), owing to smaller λ_o and larger $\Delta\lambda$ and larger mean $\overline{R}$.

15. Conclusions and six steps of forecasting

For realization of the **first step** of forecasting we need one minute real-time data from almost all NMs of the world network. On the each NM there must work automatically the program for the search of the start SEP events as it was described in Sections 1-3. This search will help to determine which NM from about 50 of total number operated in the world network shows the narrow peak of the anisotropic stream of the first arrived solar CR (NM of the 1-st type) and which shows a diffusive tail with a wide maximum at a later time (NM of the 2-nd type). In the **second step** we determine rigidity spectrum of arrived solar CR $I_S \propto R^{-\gamma_S}$ by using separately NM of the 1-st type and 2-nd type by using method of coupling functions as it was described in Section 4 (for details, see: Chapter 3 in [1]). In the **third step** we need to determine for different NMs the mean $\overline{R}$, λ_o and $\Delta\lambda$ characterizing this event. By using these parameters and experimental data on NM time profiles in the beginning time we cane determine parameters of solar CR non-scattering and diffusive propagation, described in Section 13 (the **fourth step**). On the basis of determined parameters of solar CR non-scattering and diffusive

propagation we then determine expected CR fluxes and pitch-angle distribution for total event in interplanetary space in dependence on time after ejection (the **fifth step**). In the **sixth step** by using again method of coupling functions we can determine expected radiation doze which will be obtained during this event inside space probes in interplanetary space, satellites in the magnetosphere, aircrafts at different altitudes and cutoff rigidities, for people and technologies on the ground.

REFERENCES

[1] L.I.Dorman, "Cosmic Rays in the Earth's Atmosphere and Underground", Kluwer Academic Publ., Dordrecht/Boston/London, 2004. 855 pages.

[2] L.I.Dorman, "Cosmic Ray Interactions, Propagation, and Acceleration in Space Plasmas", Springer, Netherlands, 2006. 847 pages.

[3] Yu.I.Fedorov, M.Stehlik "Description of Anisotropic Particle Pulse Transport Based on the Kinetic Equation", *Astrophys. Space Sci.,* 1997, v. 253, n. 1, pp. 55-72.

[4] Yu.I.Fedorov, B.A.Shakhov, M.Stehlik "Non-Diffusive Transport of Cosmic Rays in Homogeneous. Regular Magnetic Fields", *Astron. Astrophys.*, 1995, v.302, n. 2, pp. 623-634.

[5] Yu.I.Fedorov, M.Stehlik, K.Kudela, J.Kassovicova "Non-Diffusive Particle Pulse Transport: Application to an Anisotropic Solar GLE", Solar Phys., 2002, v. 208, n. 2, pp. 325-334.

[6] L.I.Dorman, B.A.Shakhov, M.Stehlik "The Second Order Pitch-Angle Approximation for the Cosmic Ray Fokker-Planck kinetic equations", in: Proceedings of the 28th International Cosmic Ray Conference, Tsukuba, Japan, 2003, v. 6, pp. 3535-3538.

[7] M.Lumme, M.Nieminen, J.J.Torsti, E.Vainikka, J.Peltonen "Interplanetary Propagation of Relativistic Solar Protons", Solar Phys., 1986, v. 107, n. 1, pp. 183-194.

[8] L.P.Borovkov, L.L.Lazutin, O.I.Shumilov, E.V.Vashenyuk "Injectin Characteristics of Energetic Particles on the Sun during GLE", in: Proceedings of the 20th International Cosmic Ray Conference, Moscow, Russia, 1987, v. 3, pp. 124-127.

[9] J.Kassovicova, K.Kudela "On the Computations of Cosmic Ray Trajectories in the Geomagnetic Field", Preprint IEP SAS, Kosice, 1998, pp. 1-12.

[10] L.I.Dorman, "Experimental and Theoretical Principles of Cosmic Ray Astrophysics", Physmatgiz, Moscow, 1975.

[11] P.I.Y.Velinov, G.Nestorov, L.I.Dorman, "Cosmic Ray Effects on the Ionosphere and on the Radiowaves Propagation", Publ. House of Bulg. Acad. Sci., Sofia, 1974, 312 pages.

[12] N.A.Tsyganenko. "A Magnetospheric Magnetic Field Model with a Warped Tail Current Sheet", Planet. Space Sci., 1989, v. 37, n. 1, pp. 5-20.

[13] L.I.Dorman, "Cosmic Rays in Magnetospheres of the Earth and other Planets", Springer, Netherlands, 2009, 770 pages.

[14] M.A.Shea, D.F.Smart, "Vertical Cutoff Rigidities for Cosmic ray Stations since 1955", in: Proceedings of the 27th International Cosmic Ray Conference, Hamburg, Germany, 2001, v. 3, pp. 4063-4066.